CHAPTER 2

MATERIALS AND EXPERIMENTAL METHODS

This chapter illustrates the design, melting, casting of the material, procedures for homogenization, hot-rolling, austempering, patenting treatment of the developed materials and their characterization. The microstructural characterization of materials using optical microscopy, scanning electron microscope, transmission electron microscope and electron backscatter diffraction analysis are described. Phases and their quantification, crystallite size, micro strain, dislocation density and carbon content are analyzed through X-ray diffractometer. The procedures of hardness measurement, tensile testing, low cycle fatigue testing and Charpy impact testing are described. Also, the procedures of dry sliding wear testing, electrochemical and immersion corrosion testing are presented.

2.1 DESIGN OF THE MATERIALS

Three compositions of Fe-C-Mn-Si-Cr-Mo-Co-Ni-Al based alloys were designed utilizing JMatPro database by varying carbon and Ni content to achieve martensite-start temperatures (Ms) much below, below and above room temperature (RT). The designed compositions are listed in Table 2.1.

Table 2.1 Selected compositions (by mass%).

C	Si	Mn	Cr	Mo	Al	Co	Ni	Fe	Ms
1.2	2.5	2.0	1.26	0.24	1.0	1.5	0	Bal.	<<RT
1.5	2.5	2.0	1.26	0.24	1.0	1.5	0	Bal.	<RT
0.98	2.5	2.0	1.26	0.24	1.0	1.5	0.50	Bal.	>RT

2.2 MATERIALS

2.2.1 Raw Materials

The raw materials (Fig 2.1) like ferro-carbon (Fe-C), ferro-molybdenum (Fe-Mo), Ferro-chromium (Fe-Cr), ferro-silicon (Fe-Si), ferro-manganese (Fe-Mn), aluminium, cobalt, nickel and manganese used for making designed compositions were procured from Midhani, Hyderabad and Mahindra Sanyo Special Steel Ltd. The chemical compositions of the raw materials are listed in Table 2.2.

Table 2.2 Chemical composition of the raw materials (by mass%).

	C	Si	Mn	Cr	Mo	Al	Co	Ni	Fe
Fe-C	1.25	0.25	0.35	0.25	--	--	--	0.15	Bal.
Fe-Mo	0.1	1.0	2.0	1.26	60	--	--	--	Bal.
Fe-Cr	--	0.6	0.35	70	--	--	--	0.15	Bal.
Fe-Si	0.15	70	--	--	--	1.5	--	--	Bal.
Fe-Mn	7.95	0.68	78.7	--	--	--	--	--	Bal.
Al	--	---	--	--	--	100	--	--	--
Co	--	--	--	--	--	--	100	--	--
Ni	--	--	--	--	--	--	--	100	--
Mn	--	--	100	--	--	--	--	--	--
Fe-C	1.25	0.25	0.35	0.25	--	--	--	0.15	Bal.

Figure 2.1 Raw materials used for making studied compositions.

2.2.2 Melting and Casting

Designed compositions were melted in a vacuum induction melting furnace (Fig 2.2a) of 2 kg capacity assisted with argon gas. The steps involved in melting and casting are described below:

Step 1: Raw materials like ferro-carbon, ferro-molybdenum, ferro-silicon, ferro-chromium, cobalt, nickel, aluminium except manganese and ferro-manganese are charged into the furnace and vacuum of 10^{-4} mbar is created into the melt chamber followed by power supply to the heating element starting from 0 units and kept for 10 minutes for initial heating. Further power rating is increased to 25 units in a step size of 5 units/10 minutes. As the temperature of melt reaches to 1600°C, all the material are in molten state and melt was kept at this temperature for 20 minutes for proper alloying.

Step 2: Temperature of the melt was reduced to 1575°C and argon gas was purged into the furnace till 600 mbar pressure followed by addition of manganese and ferro-

manganese to the melt and kept for 3 minutes. Argon was purged in order to avoid evaporation of manganese at high temperature and a very low pressure.

Step 3: Melt was poured at 1550°C in a Cu mold (Fig 2.2b) and after cooling cast ingot (Fig 2.3) was removed from the mold.

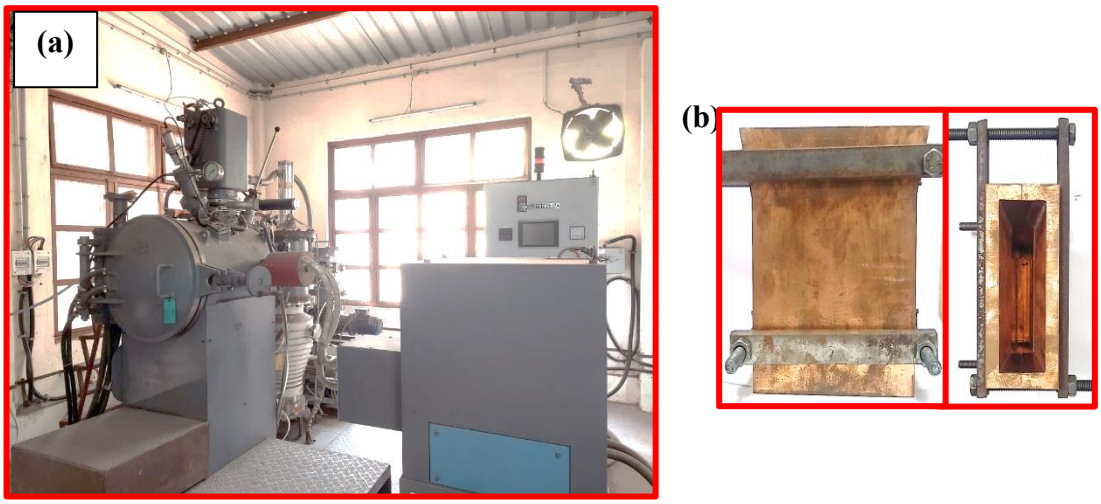

Figure 2.2 (a) Vacuum induction melting furnace and (b) copper mold.

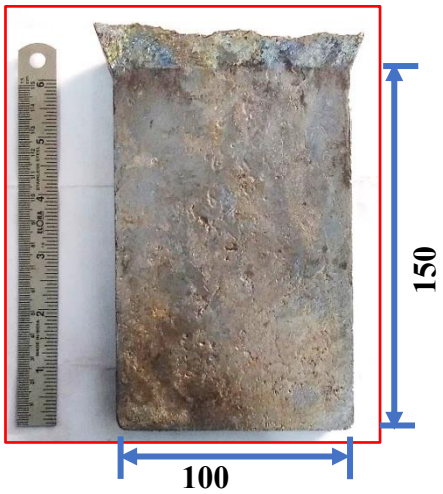

Figure 2.3 Cast ingot.

The alloy was cast as a plate of 150 mm x 100 mm x 25 mm. The cast plates were cut into the required dimensions by electrical discharge machining (wire EDM) and

homogenized at 1200°C for 24 h followed by furnace cooling (Figure 2.4). The homogenized plates (Figure 2.5) were hot rolled at 1050°C for a 75% reduction in thickness to break the cast structures (Figure 2.4). The chemical compositions of the hot-rolled plates (Figure 2.6) were analyzed with the spark atomic emission spectroscopy method according to the ASTM E-415 standard and the results are given in Table 2.3. The alloy steels were designated as B12VA, B14VA and B15VA as given in Table 2.3.

Table 2.3 Chemical composition of hot-rolled steels (by mass%).

Alloy steels	C	Si	Mn	Mo	Cr	Ni	Co	Al	Fe	Ms (°C)
B12VA	1.18	2.35	2.19	0.29	1.31	0.06	1.44	1.25	Bal.	-59
B14VA	1.02	2.29	2.14	0.25	1.38	0.05	1.40	1.19	Bal.	8
B15VA	0.97	2.2	1.69	0.22	1.42	0.43	1.39	1.13	Bal.	43

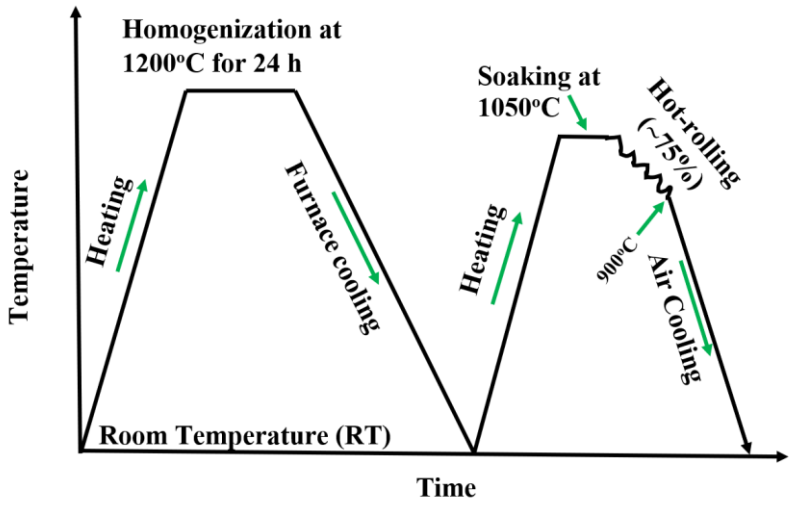

Figure 2.4 Heat-treatment cycles for homogenization and hot-rolling.

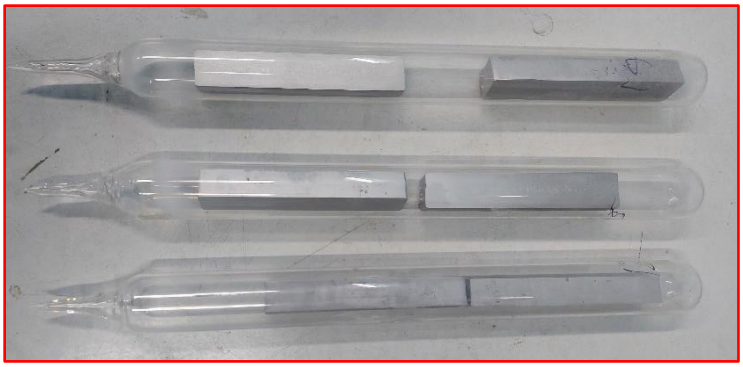

Figure 2.5 Homogenized samples vacuum sealed in quartz tube.

Figure 2.6 Hot-rolled plate (~75% reduction).

2.2.3 Calculations of Transformation Kinetics

Time-temperature austenitization (TTA) diagrams for the three alloys B12VA, B14VA and B15VA were calculated from the JMatPro software to find approximate austenitization temperature and time to achieve homogeneous austenite in the alloys and respective diagrams are given in Figure 2.7a, b, c. Time-temperature-transformation (TTT) diagrams for the selected alloys were also calculated to find austempering temperature and time to get required amount of bainite. The calculated TTT diagrams for the selected three alloys B12VA, B14VA and B15VA are shown in respective Figures 2.8 to 2.10.

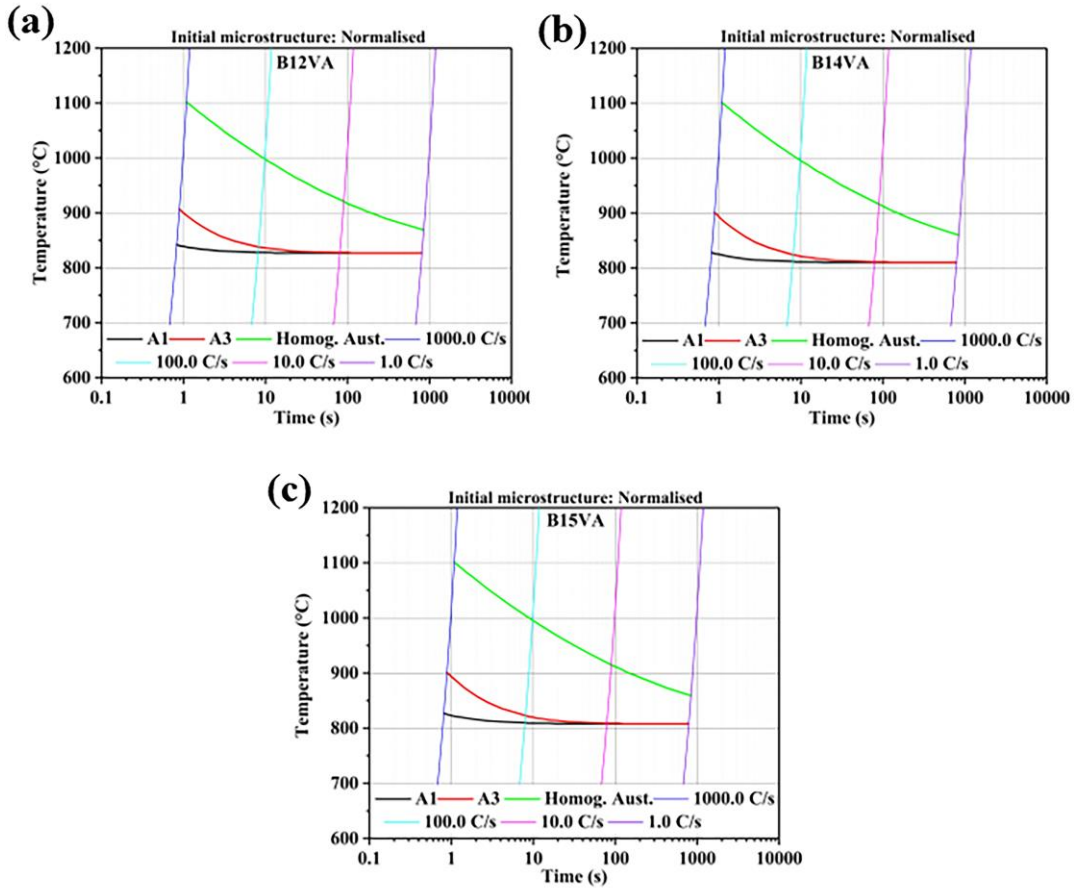

Figure 2.7 Calculated time-temperature austenitization (TTA) diagrams (a) B12VA alloy, (b) B14VA alloy and (c) B15VA alloy steels using the JMatPro database.

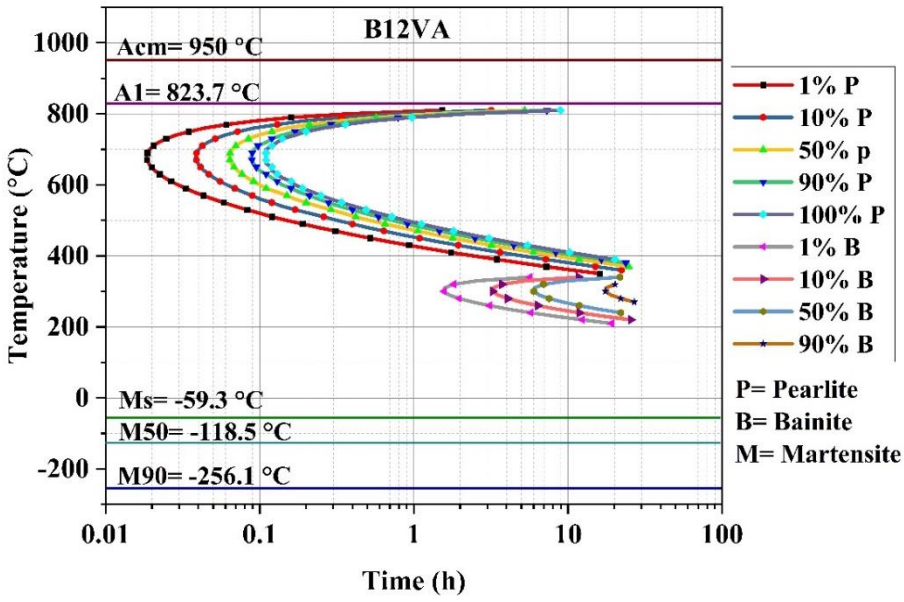

Figure 2.8 Calculated TTT diagram of the B12VA steel using JMatPro database for an austenite grain size of ASTM 8 and austenitizing temperature of 950°C.

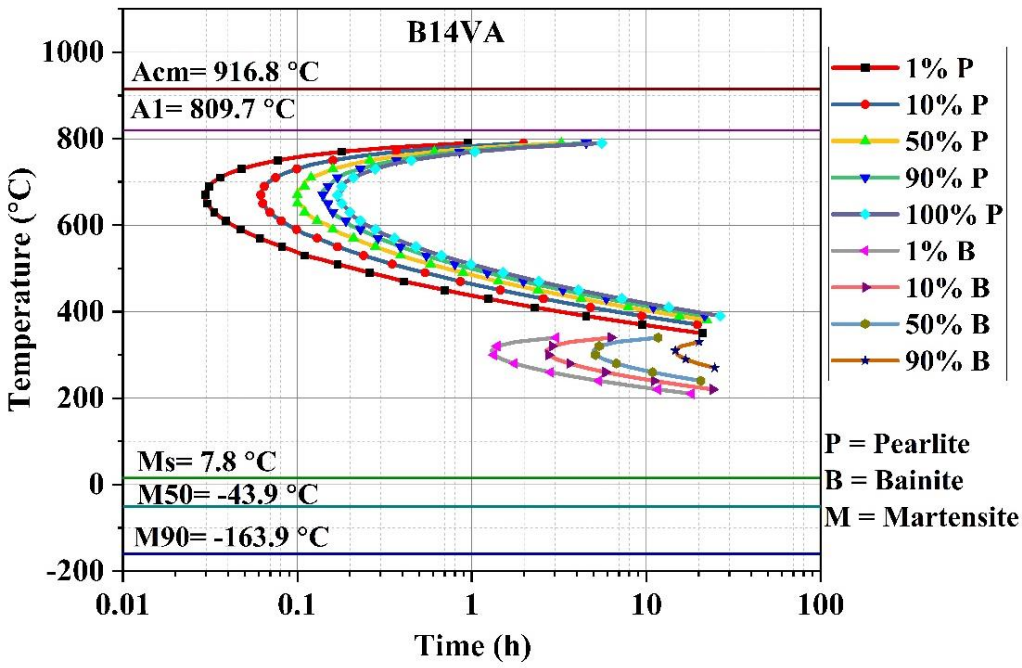

Figure 2.9 Calculated TTT diagram of the B14VA steel using JMatPro database for an austenite grain size of ASTM 8 and austenitizing temperature of 950°C.

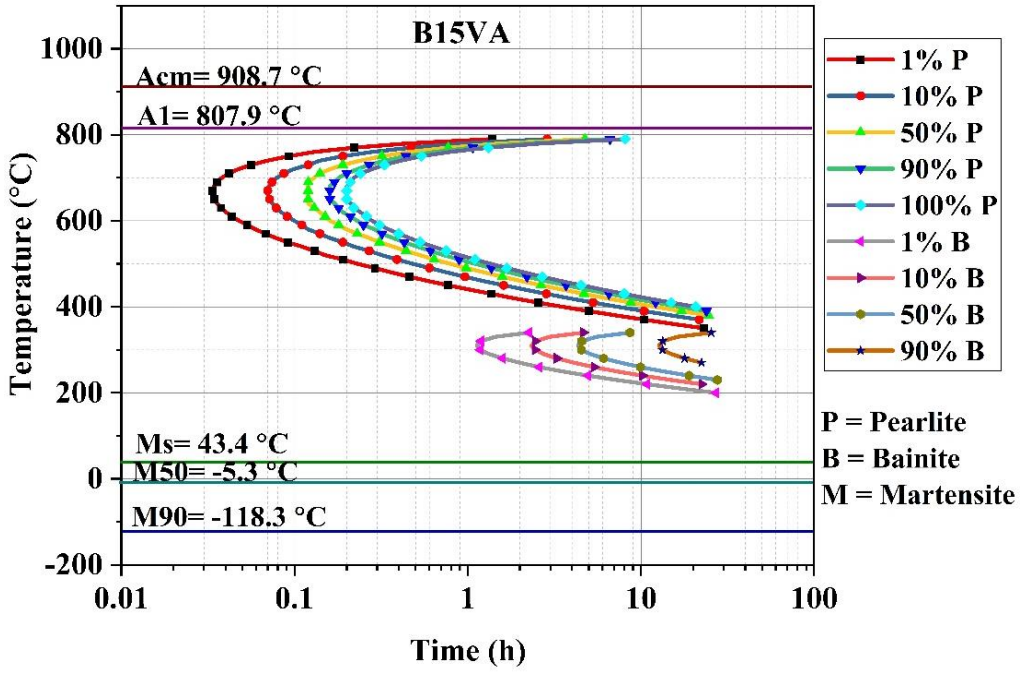

Figure 2.10 Calculated TTT diagram of the B15VA steel using JMatPro database for an austenite grain size of ASTM 8 and austenitizing temperature of 950°C.

The composition of the alloy is selected such that the martensite start temperature is maintained at a very low level such that bainite can be produced at lowest temperature. The calculated martensite starts temperature (Ms) and bainite start temperature (Bs) for the selected steel are presented in Table 2.4. The available data (transformation temperature and time of 10% and 50% transformation from the TTT diagram) were used to calculate austempering time at 250°C for different fractions of bainite using Johnson–Mehl–Avrami–Kolmogorov (JMAK) equation [137, 138] (Equation (2.1)). The austempering temperature is kept at a reasonably low temperature (250°C) to get fine bainite to achieve better mechanical properties. The fraction of isothermal transformation product (f) is given by

$$f = 1 - \exp\left(k'' t^m\right) \tag{2.1}$$

Where t is the isothermal transformation time, k″ and m are rate constants and JMAK's exponent, respectively. The loss in transformation kinetics due to low austempering temperature is compensated by addition of the required amount of Co and Al which accelerate kinetics. Therefore, in the present investigation, the heat treatment schedule is designed such that partial transformation of austenite to nanostructured bainite could be obtained at a significantly low timing. The austempering times to get 52% and 65% bainite in B12VA were 72 h and 96 h, respectively and the corresponding bainitic steels were designated as B12VA-1 and B12VA-2. Similarly, the Austempering times to produce 33% and 65% bainite in B14VA were 24 h and 48 h, respectively and the corresponding bainitic steels were named as B14VA-1 and B14VA-2. The calculated Austempering times to make 55% and 65% bainite in B15VA were 18 h and 50 h, respectively and the corresponding bainitic steels were denoted as B15VA-1 and B15VA-2.

Table 2.4 Transformation time for different fraction of bainite.

Alloys	Tr Time (h)	V_B (%)	Ms (°C)	Bs (°C)
B12VA-1	72	52	-59	353
B12VA-2	96	65		
B14VA-1	24	33	8	357
B14VA-2	48	65		
B15VA-1	18	55	43	360
B15VA-2	50	65		

2.2.4 Heat Treatment

2.2.4.1 Austempering Treatment

In an evacuated quartz tube, 100 x 15 x 2.5 mm^3 hot-rolled plates were austenitized at 950°C for 30 minutes. All the austentized samples were transferred from the quartz tube to a molten salt bath (mixture of $NaNO_3$ and KNO_3 in a 1:1 ratio) maintained at 250°C. Hot-rolled plates were austempered (Figure 2.11) at 250°C for varying durations to get the required amounts of bainite.

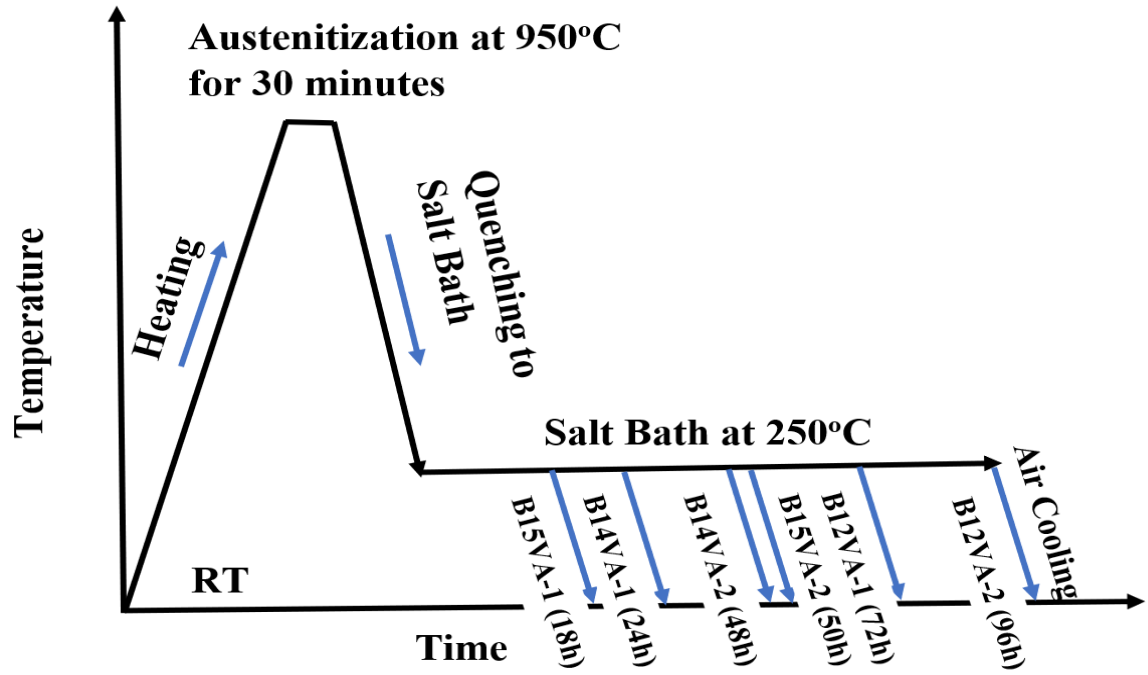

Figure 2.11 Austempering heat-treatment cycles of the hot-rolled steels.

2.2.4.2 Patenting

Hot-rolled plates of all three alloys B12VA, B14VA and B15VA were also patented (Figure 2.12) at 550°C for 1 h followed by furnace cooling to achieve 100% fine pearlite and the corresponding pearlitic steels were designated as P12VA, P14VA and P15VA, respectively.

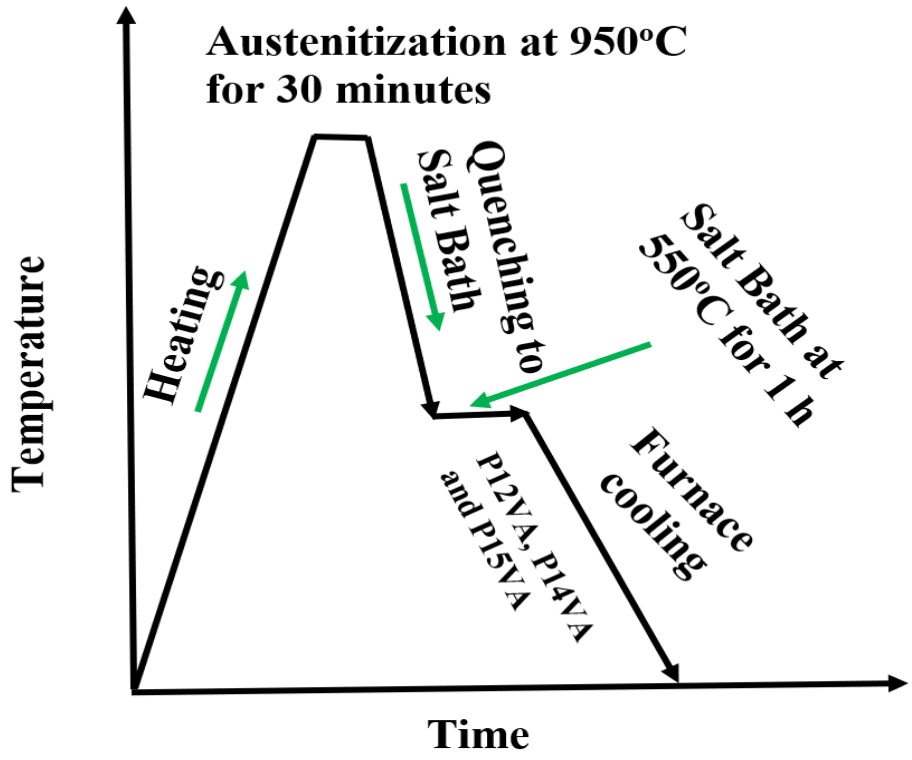

Figure 2.12 Patenting heat-treatment cycles of the hot-rolled steels.

2.3 MICROSTRUCTURAL CHARACTERIZATION

2.3.1 Optical Microscopy (OM)

The optical microscopy is used to observe morphology and distribution of bainite, austenite and pearlite. Austempered and patented hot rolled plates were machined to 2 mm to remove a decarburized layer, if any. 12 x10 x 2 mm^3 sized samples were cut from the austempered and patented plates. Cut samples were ground using SiC abrasive papers upto 2500 grit size and mechanically polished by cloth with diamond paste and diamond

aerosol. Polished specimens were chemically etched with 2% nital solution. Microstructural characterization was carried out using a "Leica DFC-295" optical microscope.

2.3.2 Scanning Electron Microscopy (SEM)

The scanning electron microscope (SEM) is used to characterize morphology of bainite, retained austenite, pearlite, and size of blocky austenite. Polished samples were lightly etched with 2% nital solution and microstructural characterization was done using a "Nova Nano SEM 450" FE-SEM operated at 20 kV. The size of blocky austenite is measured by linear intercepts in random directions for at least 50 blocks in SEM secondary electron images and an average value is reported. Surface morphology of worn samples and corroded samples were also investigated in SEM. Worn out and corrosion products were characterized using SEM energy dispersive spectroscopy (EDS). Fracture behaviour of the samples tested under tensile, Charpy impact and cyclic loading was also examined using SEM. Fracture ends of ~4 mm length of the tensile, Charpy impact and fatigue tested samples were sectioned transversely and cleaned ultrasonically in acetone before SEM analysis.

Samples of dimension 12 mm x 10 mm x 2 mm are mechanically polished and then subjected to final polishing step using colloidal silica of 0.3 μm size in a vibroMet. The polished samples are then scanned for electron back-scattered diffraction (EBSD) study using a Quanta 3D FEG SEM at an accelerating voltage of 20 kV, a working distance of 16 mm, and a tilting angle of 70°. The step size and scan areas are 70 nm and 70 μm x 70 μm respectively. The scanned data is cleaned with a grain tolerance angle lower than 2° and a confidence index lower than 0.1. The cleaned data is then used to generate Image quality (IQ), Inverse pole figure (IPF) map, Kernel average misorientation (KAM) and phase maps using TSL OIM software version 8.

2.3.3 Transmission Electron Microscopy (TEM)

TEM study was carried out to characterize morphology, size and its distribution of bainite and filmy austenite, carbides if any, ferrite, cementite and analysis of selected area diffraction pattern (SADP) was done for confirmation of phases. Thin slices of 500 μm thickness were cut from the heat-treated samples using a slow-speed diamond cutter and mechanically ground to 40 μm thickness foil using 220, 400, 600, 800, 1000,1500 and 2500 grit size SiC abrasive papers. A 3 mm diameter disc was punched from the foil. The discs were electrolytically thinned down to perforation by "Struers Tenupol-5" Twin jet elctropolisher using electrolyte of 60 vol % methanol, 34 vol % n-butanol and 6 vol % perchloric acid at 18 V and temperature of 231 K. Detailed microstructure of electropolished samples were studied by Tecnai G^2 20 TWIN transmission electron microscope (TEM), operating at 200 kV. TEM analysis of tensile fractured samples were carried out in order to note any microstructural changes during static and cyclic loading. Also, TEM analysis of sub-surfaces was done to observe microstructural changes resulting from wear.

The intercept thickness was measured in the direction perpendicular to the longitudinal dimension of the bainite plate or austenite film in TEM bright-field images using Image-J software. The measurement was carried out randomly on 150 to 200 plates or films and mean intercept thickness was reported. The measured mean intercept thickness of the bainite/austenite plate or film was corrected by multiplying a stereological factor of $2/\pi$ [139].

2.3.4 X-ray Diffraction

The X-ray diffractometer is used to find phases and its quantification, crystallite size, micro strain, dislocation density and carbon content of retained austenite. Polished

heat-treated samples were also scanned in Rigaku Smart Lab 9kW, high resolution (HR) X-ray diffractometer with monochromatic Cu K_α radiation (1.54 Å) operated at 40 kV and 40 mA at 2°/min scan rate with 0.001° step size in the 2θ angular range of 40° to 95°. The (111), (200), (220) and (311) peaks of austenite and the (110), (200) and (211) peaks of bainitic ferrite were used to minimize the standard error in the x-ray diffraction (XRD) peaks.

2.3.4.1 Identification of Phases

The phases were identified from the corresponding JCPDS card number as follows:

- Bainite- JCPDS card number: 00-006-0696
- Retained austenite- JCPDS card number: 01-081-8775
- Ferrite- JCPDS card number: 00-006-0696
- Cementite- JCPDS card number: 00-035-0772
- Martensite-
    - BCT- JCPDS card number: 00-044-1293
    - HCP- JCPDS card number: 01-071-4408

2.3.4.2 Quantification of Phases

The area under the peaks was measured using X'Pert Highscore Plus software. The volume fraction of retained austenite (V_{RA}) was calculated by dividing the sum of the areas of all peaks of retained austenite (RA) by the sum of the areas of all peaks of bainite and retained austenite using Equation (2.2) [51]. The volume percent of RA (V_{RA}) was calculated

$$V_{RA} = \frac{\sum_{i=1}^{n} A_\gamma}{\sum_{i=1}^{n} A_\gamma + \sum_{i=1}^{n} A_{\alpha_b}} \quad (2.2)$$

Here, A_γ and $A_{\alpha b}$ represent the area of the austenite and bainite peaks, respectively. The volume percent of bainite was also estimated using a similar principle.

The ratio of volume fraction of film-like retained austenite to blocky retained austenite was estimated using Equation (2.3) [140].

$$\frac{V_{RA}^{F}}{V_{RA}^{B}} = \frac{0{\cdot}15V_{BF}}{V_{RA}-0.15V_{BF}} \quad (2.3)$$

Where V_{RA}^{F} is the volume fraction of filmy retained austenite, V_{RA}^{B} is the volume fraction of blocky retained austenite and V_{BF} is the volume fraction of bainitic ferrite. The volume fractions of filmy and blocky austenite were calculated from their ratio and total fraction.

2.3.4.3 Crystallite Size, Lattice microstrain and Dislocation Density

The Scherrer formula was used to compute the crystallite size, lattice microstrain of bainite and austenite of major XRD peaks using the corrected Lorentzian and Gaussian components of integral breadth widths [141] (Equation (2.4) & Equation (2.5)).

$$B = \frac{k^{o}\lambda}{\beta_{size}.Cos\theta} \quad (2.4)$$

$$\beta_{strain} = 4\varepsilon_R tan\theta \quad (2.5)$$

The two broadening parameters β_{size} and β_{strain} in these equations represent adjusted integral breadth owing to crystallite size and lattice strain, respectively. Here symbol B denotes crystallite size, k^{o} is the Scherrer constant, ε_R is the lattice microstrain and λ is the wavelength of X-ray used. From the crystallite size and lattice microstrain on the (110) plane, the dislocation density of bainite was estimated using Equation (2.6) [142, 143].

$$\rho_{110} = \frac{2\sqrt{3}\cdot\langle\varepsilon^2_{R110}\rangle^{1/2}}{B_{110}\cdot b} \quad (2.6)$$

Where ρ is dislocation density and the suffix 110 indicates reflections from the (110) plane. Symbol b denotes the Burgers vector of dislocation and its numerical value is 2.48 nm for BCC iron. The dislocation density of retained austenite was calculated in similar principle with Burgers vector of 2.57 nm.

2.3.4.4 The Carbon Content (C_Υ) of the Retained Austenite

The carbon content (C_Υ) of the retained austenite was calculated using composition dependent lattice parameter given by Equation (2.7) [144] and the measured lattice parameter (a_Υ) from the X-ray diffraction data.

$$a_\Upsilon = 3.5780 + 0.033C_\Upsilon + 0.00095Mn - 0.0002Ni + 0.0006Cr + 0.0031Mo + 0.0018V \quad (2.7)$$

Further to observe any phase transformation during tensile straining, Charpy impact testing and cyclic loading detailed investigation was performed using x-ray diffraction.

2.4 MECHANICAL PROPERTIES

Mechanical properties were evaluated by Vickers hardness measurement, tensile testing, Charpy impact testing, and low cycle fatigue testing.

2.4.1 Hardness

The hardness measurement was carried out on polished heat-treated samples of dimension 12 x10 x 2 mm^3 using the "Leco-700 model" Vickers hardness tester at a load of 10 kgf and a dwell time of 10 seconds. Average hardness data of 10 indentations were reported with a standard deviation. The Vickers microhardness at 50 gf load for 10 s was used on the cross-section of worn surfaces by microhardness tester (model: Leco LM 248AT).

2.4.2 Tensile Tests

Oversized tensile samples were cut and machined from austempered and patented plates to dimensions of gauge length of 25 mm, gauge width of 6 mm, thickness of 2 mm and overall length of 100 mm (Figure 2.13) to eliminate the decarburization effect, if any. Heat-treated subsized tensile samples were ground and polished. Tensile tests of polished subsize samples were performed at room temperature at a cross-head speed of 0.5 mm/minute (approx. strain rate of $3.3x10^{-4}$ s^{-1}) by "Instron 5982" Universal testing machine of 100kN capacity according to ASTM E8-E8M-22 standard [145]. The tensile testing of all the samples was done mounting an extensometer of gauge length of 10 mm. To ensure repeatability of tensile results, 3 tests were performed for each condition. Average values of strength and ductility are reported with standard deviation.

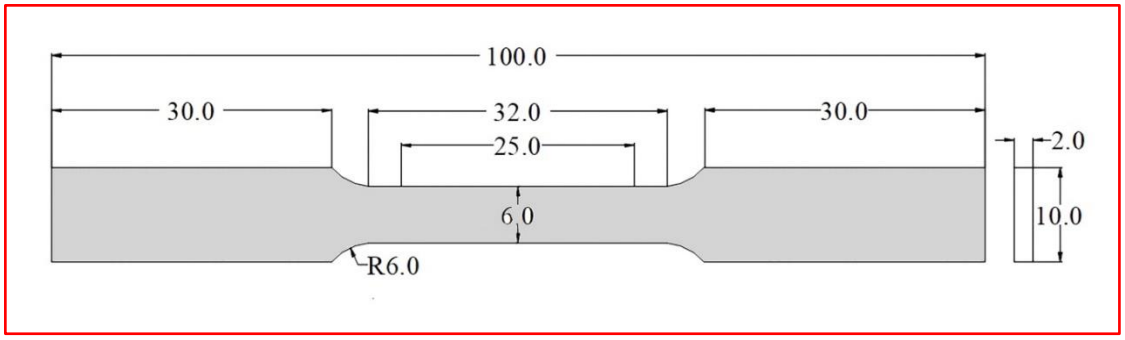

Figure 2.13 Geometry of the tensile sample (all dimensions in mm).

2.4.3 Low Cycle Fatigue tests

Austempered blanks of B12VA-2, B14VA-2 and B15VA-2 were machined into fatigue samples of gauge length of 15 mm and gauge diameter of 5.5 mm as shown in Figure 2.14. The gauge section of samples was mechanically ground with emery papers up to 2500 grit size to remove machining marks, if any. Final cloth polishing was done using 0.5-1 µm diamond paste and diamond aerosol lubricant. A MTS^{TM} servo-hydraulic machine (Model 810) of 50 kN capacity, equipped with fully automatic Flex Text 40

controller was used to conduct total strain controlled low cycle fatigue (LCF) tests on standard sample as per ASTM E606 standard with fully reversible (R = –1) axial loading with triangular waveform (Figure 2.11). All the tests were repeated to ensure reproducibility of results.

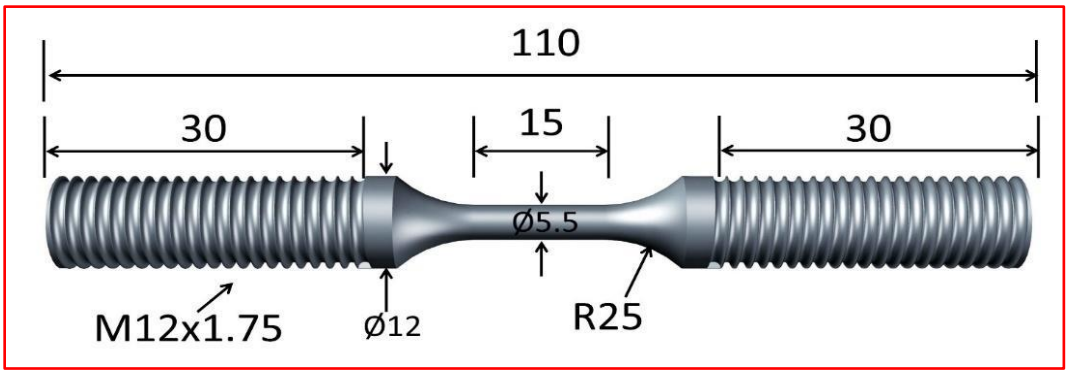

Figure 2.14 Geometry of LCF test sample (all dimensions in mm).

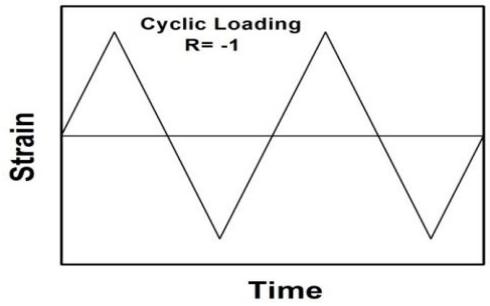

Figure 2.15 Triangular Waveform.

LCF tests were conducted at total strain amplitudes of ±0.50%, ±0.60%, ±0.70% and ±0.80% at a fixed strain rate of 0.005 s^{-1}. The test matrix of low cycle fatigue tests is shown in Table 2.5. Cyclic strain was controlled by mounting an extensometer of 10 mm gauge length (Model: MTS 632.13C-20) on gauge section of the fatigue samples. The elastic, plastic and total strain components along with stress amplitudes, both in tensile and compressive part of each fatigue cycle, were displayed and stored during test by the controller software attached to the machine. The fractography of the fatigue-tested samples was carried out using scanning electron microscope.

Table 2.5 Test matrix for Low cycle fatigue tests.

SR. No.	Samples	Total strain amplitudes (%)	Strain rate (s^{-1})
1	B12VA-2	±0.50, ±0.60, ±0.70 and ±0.80	$5x10^{-3}$
2	B14VA-2		
3	B15VA-2		

2.5 CHARPY IMPACT TESTING

Oversized samples of dimensions 10.5x10.5x55.5 mm^3 were cut from austempered blanks of B12VA-1, B12VA-2, B14VA-1, B14VA-2, B15VA-1 and B15VA-2 utilizing wire EDM. Samples were ground and polished to dimension 10x10x55 mm^3 followed by V-notch preparation using wire EDM according to ASTM E23-18 standard. Notch was cut at 45° angle with tip radius of 0.25 mm and 2 mm notch depth. and subsequent grinding and polishing were carried out, with particular attention given to the careful polishing of the notch section. Charpy samples were tested using an Instron® SI-1C3 model instrumented impact testing machine (400 J capacity), attached with Instron Dynatup Impulse data acquisition system, at -40°C, 0°C and room temperature. The sample temperature was continuously monitored by a thermocouple and was maintained within ±2 °C using a medium of methanol and liquid nitrogen.

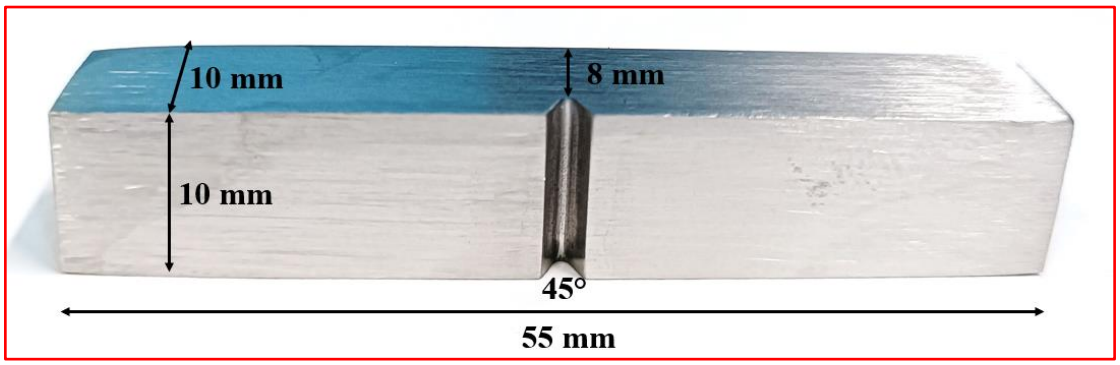

Figure 2.16 Charpy impact samples as per ASTM E23-18 standard (all dimensions are in mm).

2.6 PIN-ON-DISC WEAR TESTING

Oversized cylindrical pins were machined from austempered and patented blanks by wire EDM. Heat-treated cylindrical pins were ground using SiC papers till 2500 grit size and the surface roughness were measured utilizing surface roughness tester (model: Mitutoyo SJ-410). The average value of five tests along with standard deviation are reported. A counter disc made of tungsten carbide with hardness of 1700 HV was utilized for pin-on-disc dry sliding wear test. The tungsten carbide disc was used in order to avoid the loss of counter disc material sliding against high hardness bainitic pins. Numerically controlled pin-on-disk dry sliding wear tests were conducted at varying applied normal loads of 10 N, 20 N, 30 N, 40 N and 50 N and sliding distances of 1500 m, 3000 m, 4500 m and 6000 m with constant angular and sliding velocity of 273 rpm and 1m/s, respectively using Magnum pin-on-disc tester as per ASTM G99-17 standard [146]. The parameters of tribological studies are reported in Table 2.6.

Table 2.6 Test parameters of tribological studies of austempered and patented steels.

Test parameters	
Counter disc material	Tungsten carbide
Normal loads (P)	10 N, 20 N, 30 N, 40 N and 50 N
Sliding distances (D)	1500 m, 3000 m, 4500 m and 6000 m
Angular velocity of disc	273 rpm
Sliding velocity	1 m/s
Pin diameter	6 mm
Track radius	35 mm

The mass losses after wear test were measured in Metler Toledo balance (model: ME204) with a resolution of 0.1 mg. The specific wear rate (W_{sp}) for studied steel at normal loads of 10 N, 30 N and 50 N with varying sliding distance from 1500 m to 6000 m were calculated by utilizing Equation (2.8) [147].

$$W_{sp} = \frac{V}{DP} \quad (2.8)$$

Where, V is the volume loss (mm^3), D is the sliding distance (m) and P is normal load (N).

The time variation in friction coefficient curves were observed for each wear test in order to know wear regime and nature of contact surfaces.

The Stylus profile surface roughness tester and the Atomic Force Microscopy (AFM) were utilized in order to assess the surface roughness of the wear tested samples. Also, peaks and valleys of worn surfaces were observed by AFM. SEM along with EDS analysis was utilized to characterise the wear mechanism of the steel. To observe strain-hardening effect, the Vickers microhardness at 50 gf load was used on the cross-section of worn surfaces by microhardness tester (model: Leco LM 248AT). TEM analysis of sub-surfaces was done to observe microstructural changes resulting from wear.

2.7 CORROSION TESTING

Corrosion behaviour of indigenously developed high carbon high silicon carbide-free nanostructured bainitic steels was studied with electrochemical and immersion corrosion in an aqueous 3.5% NaCl solution and corrosion behaviour is compared with the pearlitic steel of the same compositions. Samples of 15x15x2 mm^3 and 10x10x2 mm^3 dimensions were cut from heat-treated plates for electrochemical measurement and immersion corrosion test, respectively.

2.7.1 Electrochemical Corrosion Tests

The samples for corrosion study were ground utilizing SiC papers up to 2500 grit size before being cloth-polished using diamond spray lubricant and paste. The electrochemical corrosion behaviour of polished bainitic and pearlitic steels, was studied

with open circuit potential (OCP), electrochemical impedance spectroscopy (EIS) and potentiodynamic polarization using CORRTEST CS350 potentiostat (Figure 2.17). The tests were conducted in an aqueous 3.5 wt.% NaCl solution at room temperature (RT). For all electrochemical measurements, a flat cell with three electrodes consisting of a working electrode (bainitic and pearlitic steel), reference electrode (Ag/AgCl), and platinum grid as counter electrode were utilized. 1 cm^2 area of the polished sample was exposed to the solution during an electrochemical test.

Figure 2.17 Potentiostat with flat cell having three electrode system.

Primarily, the OCP test was conducted for 2 h to stabilize the cell potential, which was followed by an EIS test conducted in the frequency range of 0.01 Hz to 100000 Hz with ±10 mV amplitude with respect to OCP. The CS-studio program was utilized to fit the impedance data with the R(CR) electrical equivalent circuit. The electrochemical potentiodynamic polarization experiments were conducted at a scan rate of 0.166 mV/s and a scan range of -250 to 500 mV relative to OCP. The corrosion current densities (i_{corr}) of the steels were calculated using Tafel extrapolation. With reference to ASTM G102-89 standard, the rate of corrosion was computed using the Equation (2.9) [148].

$$Corrosion\ rate\ = 3.27x10^{-3}x\frac{i_{corr}\,x\,Eq.Wt.}{\rho} \quad (2.9)$$

Here, i_{corr} is the corrosion current density (in μA/cm^2), ρ is the density of steel (assumed to be 7.86 g/cm^3) and Eq. Wt. is the equivalent weight of steel.

The equivalent weight of the studied steel was calculated by using Equation (2.10) [148].

$$Eq.Wt. = \left(\sum\frac{f_i z_i}{M_i}\right)^{-1} \quad (2.10)$$

Where, f_i, z_i and M_i are mass fraction, electron exchanged and atomic weight of i^{th} element, respectively. The data of Fe (2+), C (4+), Mn (2+), Si (4+), Al (3+), Co (2+) are utilized for calculation. Contribution from remaining elements is neglected due to much less than 1 mass %. The calculated equivalent weights of the selected steels are 23.2g, 23.5g and 23.7g for B12VA, B14VA and, B15VA, respectively.

The polarization resistance (R_p) of the austempered and patented steels was evaluated by utilizing CS studio program of linear RP fit within scan range of ±20 mV using Tafel data with reference to OCP. According to ASTM G102-89 [148], the R_p value was evaluated from the slope of the corrosion potential with the overpotential equal to zero, using Equation (2.11).

$$R_P = \left(\frac{\Delta E}{\Delta i}\right)E = E_{corr} \quad (2.11)$$

Where, ΔE is overpotential and Δi represents the change in current density. Each electrochemical test was performed three times and average value is reported.

2.7.2 Static Immersion Corrosion Tests

Two working surfaces of the heat-treated samples of 10 x 10 x 2 mm^3 dimension were ground up to 2500 grit size SiC papers and polished, followed by ultrasonic cleaning. Other than the exposed surface (10x10 mm^2), all other faces of the cleaned

samples were coated with a non-corrosive conventional lacquer which is insoluble in an aqueous 3.5% NaCl solution. All heat-treated coated samples were immersed at RT in an aqueous 3.5% NaCl solution (Figure 2.18). Immersion test is performed for three identical samples for 30 days by submerging them in separate 250 ml beakers to check reproducibility. After completion of the test, the samples were taken from the beakers carefully and dried at RT. The surfaces of all corroded samples were studied using scanning electron microscopy (SEM) combined with energy dispersive spectroscopy (EDS) to examine the morphology and corrosion product.

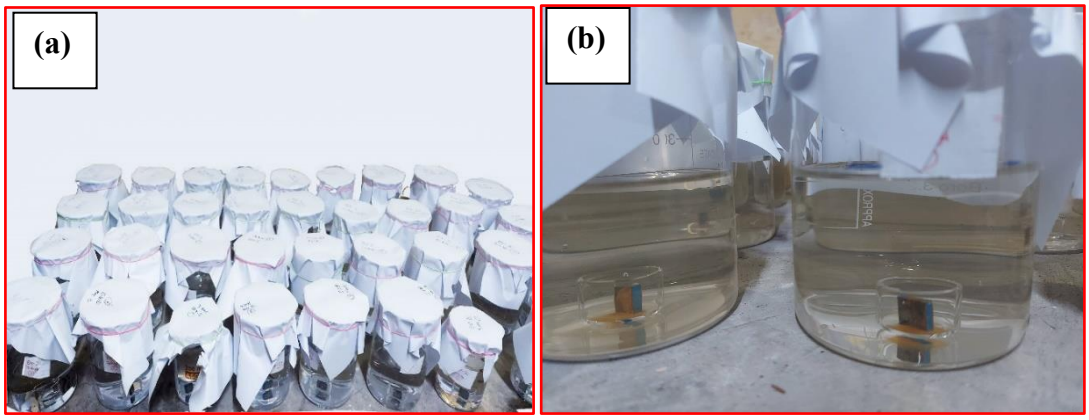

Figure 2.18 (a) & (b) Static immersion corrosion tests in an aqueous 3.5% NaCl solution.

After removing the corrosion product from the corroded surfaces, the samples were cleaned with reference to ASTM-G1-03 standard [123] utilizing Clark's reagent and weight loss was determined using a digital weighing machine (Mettler Toledo ME204). As per the ASTM G31-72 standard [149], the corrosion rate was computed using Equation (2.12).

$$Corrosion\ rate = \frac{3.154x10^{8}x\Delta w}{A\rho t} \qquad (2.12)$$

Where, Δw is the weight loss (g), ρ is the density of steel sample (g/cm^3), A is the exposed surface area (cm^2), and t is the immersion period (s).

The products of corrosion after 30 days of immersion were analysed by X-ray photoelectron spectroscopy (XPS) (Thermo Fisher Scientific K-alpha system) utilizing a monochromatic K_α source at 1400.0 eV. The C_{1s} peak at 284.8 eV was used as a reference to adjust the binding energy (BE) scale. Typically, a Gaussian component was utilized for curve fitting, while the Shirley baseline approach was employed for background removal [150].